Balejeikova, L.; Kovac, J.; Haramus, V.M.; Avdeev, M.V.; Petrenko, V.I.; Almasy, L.; Kopcansky, P.:
Influence of synthesis temperature on structural and magnetic properties of magnetoferritin.
In: Mendeleev Communications. Vol. 29 (2019) 3, 279 - 281.
First published online by Elsevier: 07.06.2019

https://dx.doi.org/10.1016/j.mencom.2019.05.012

Influence of Synthesis Temperature on Structural and Magnetic Properties of Magnetoferritin

Lucia Balejčíková[a,b]*, Jozef Kováč[b], Vasil M. Garamus[c], Mikhail V. Avdeev[d], Viktor I. Petrenko[d,e], László Almásy[f,g], Peter Kopčanský[b]

[a] Institute of Hydrology, Slovak Academy of Sciences, Dúbravská cesta 9, 841 04 Bratislava, Slovakia
[b] Institute of Experimental Physics, Slovak Academy do Sciences, Watsonova 47, 040 01 Košice, Slovakia
[c] Helmholtz-Zentrum Geesthacht: Centre for Materials and Coastal Research, Max-Planck-Street 1, 21502 Geesthacht, Germany
[d] Joint Institute for Nuclear Research, Joliot-Curie 6, 141980 Dubna, Moscow Region, Russia
[e] Taras Shevchenko National University of Kyiv, Volodymyrska Street 64, Kyiv 01033, Ukraine
[f] State Key Laboratory of Environment-Friendly Energy Materials, Southwest University of Science and Technology, Mianyang 621010, China
[g] Institute of Solid State Physics and Optics, Wigner Research Centre for Physics, Hungarian Academy of Sciences, H-1525, Budapest POB 49, Hungary

Abstract.
The regulation of synthesis temperature allows the production of artificial ferritins with different structural and magnetic properties, size distribution and colloidal stability. We studied the effect of synthesis temperature on the core structure and stability of protein shell by small-angle neutron scattering, small-angle X-ray scattering, SQUID magnetometry, dynamic light scattering and zeta potential measurements. Our results recommend the optimal temperature of synthesis of artificial ferritin for biomedical imaging applications at around 60 °C, close to the protein denaturation temperature.

***Corresponding author:** Lucia Balejčíková, e-mail: balejcikova@saske.sk

Iron is one of the essential elements for living organisms. However, an excess of iron ions is toxic, and therefore they are stored in the cavity of a spherical protein, named ferritin. Ferritin shapes as a hollow spherical shell with an external diameter of 12 nm and 2 nm thick. Functional ferritin, according to the specific requirements of each organism, could bind up to 4500 iron atoms arranged in a crystal structure similar to ferrihydrite mineral[1]. It was shown that the empty ferritin structure (apoferritin) can also be used for the chemical synthesis of other types of mineral cores composed of various metal ions (Cu^{2+}, Mn^{2+})[2,3]. In specific physicochemical conditions, it is possible to prepare artificial ferritin with unique superparamagnetic properties, e.g. magnetoferritin (MFer), which can be useful in various biomedical applications (e.g. a contrast agent in radiology, a drug carrier in targeted transport, or a standard in diagnostics of various diseases)[4,5]. The MFer synthesis protocol was derived from the general scheme of preparation of pure magnetic nanoparticles, which is based on the co-precipitation of Fe^{2+} and Fe^{3+} salts at a high temperature (50 - 80°C) in alkaline conditions (pH 8). The high thermal stability of apoferritin[6] makes this protein well suited for the synthesis of magnetic nanoparticles within its hollow core by slow addition of Fe^{2+} ions followed by controlled addition of oxidant in anaerobic conditions[7]. MFer was studied in many works using different physical methods such as magnetometry, electron microscopy, atomic force microscopy, Mössbauer spectroscopy, etc.[4,7,8]. The latest results obtained by small-angle X-ray (SAXS) and neutron scattering (SANS)[9,10] reveal a partial destruction of

the MFer protein shell with a loading factor (LF) above ~150 in comparison with a pure apoferritin shell (loading factor – the average number of iron atoms per one protein biomacromolecule) as well as aggregation of MFer molecules and sedimentation of the solutions at LF > 600. This degradation is most probably caused by iron binding or formation of a magnetic core in the protein shell[9-11]. In order to understand the protein shell destruction, the influence of pH was studied using SAXS[12]. The highest stability of MFer biomacromolecule was observed at pH 7-9, while at pH below 6 the protein shell decomposed[12]. This means that pH in the synthesis process did not affect the shell stability. The exact reason of the degradation after synthesis has not been fully understood, and in particular, the effect of synthesis temperature on the chemical composition and magnetic properties of the inorganic core as well as on the structure of the protein shell has not been investigated.

Our present study shows that synthesis temperature plays a crucial role in the development of the protein shell structure *in vitro*, the iron binding and magnetic character of magnetoferritin. Using small-angle scattering techniques, we observed a significant influence of synthesis temperature on the structure of MFer prepared with a similar amount of embedded iron oxide.

The DLS measurements reveal the variation of the average hydrodynamic diameter ($<D_{HYDR}>$) of the nanoparticles as a function of LF and synthesis temperature (Figure S1) in comparison with pure apoferritin (12.21 nm). Higher LF (640 – 940) was characterized by higher $<D_{HYDR}>$. This effect was also observed in our previous studies[9,10] and points to the impact of LF on the structure and stability of MFer solutions. It was shown that synthesis temperature affects the size of nanoparticles. A similar effect can be seen when comparing pure apoferritin and pure apoferritin heated for 100 min at 65 °C. Zeta potentials of all samples were negative and varied between -22 and -29 mV, indicating that all samples show sufficient colloidal stability (Figure S1) .

The magnetic measurements of artificial ferritins reveal the superparamagnetic behavior of nanoparticles (Figure 1). While samples with lower LF and synthesis temperature exhibit relatively weak magnetization, the curve for the highest LF prepared at 75°C shows saturation of about 14 emu/g (Figure 1). We assume that the reason for this difference is related to the formation of nano-sized magnetite/maghemite nanocrystals[8]. At lower synthesis temperatures predominantly ferrihydrite-like minerals are formed similar to those in natural ferritin[13].

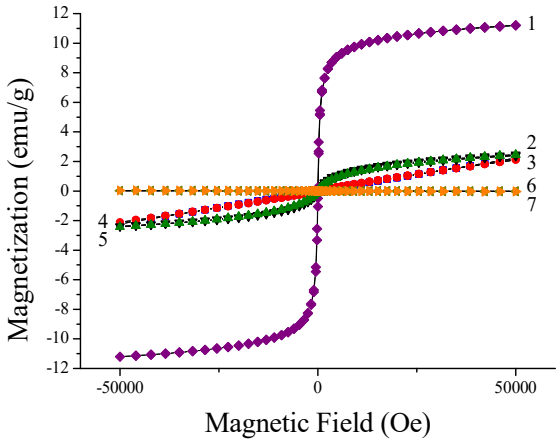

Figure 1 Room temperature magnetization curves of magnetoferritin (MFer) samples prepared at various synthesis temperatures with different loading factors in comparison with apoferritins. (1) represents MFer with LF 940 prepared at 75°C, (2) MFer with LF 660 prepared at 65°C, (3) MFer with LF 810 prepared at 55°C, (4) MFer with LF 640 prepared at

37°C, (5) MFer with LF 730 prepared at 23°C, (6) apoferritin heated at 65°C for 100 min and (7) pure apoferritin solution.

SANS curves of freeze dried MFer samples dissolved in D_2O with a protein concentration of 6 mg/ml, prepared with high iron loading at different synthesis temperatures are shown in Figure 2. Scattering maxima and minima characteristic for core-shell structure type were observed for MFer with the synthesis temperature in the range of 23 - 37 °C. The particle aggregation observed at a typical q-range below 0.2 nm^{-1} is associated probably with strong iron binding as was reported previously[9,10]. In this case, the effect of the synthesis temperature on the MFer structure is masked by strong aggregation. The SANS curves for MFer with higher LFs (640 - 940) synthesized in the temperature range from 23 to 75°C, demonstrate a loss of the core-shell structure with increasing synthesis temperature and rising LF, respectively. Despite relatively high LF of 730 and 640, the core-shell structure of MFer was preserved only at the synthesis temperatures of 23 and 37°C. At the synthesis temperatures of 55°C (LF 810) and 65°C (LF 660) the effect of LF was stronger than the effect of synthesis temperature. The increase in the scattering intensity at $q < 0.7$ nm^{-1} for all mentioned samples shows a fraction of aggregated particles. The impact of the highest synthesis temperature 75°C (near the protein denaturation temperature limit ~ 80°C [6]) was masked by the effect of the high LF 940, which was observed in our previous work[10] for high LFs, that is, the formation of large aggregated nanoparticles that sedimented before the SANS measurements. Therefore the SANS data of this sample are similar to the data for pure apoferritin. The undeniable effect of the synthesis temperature is seen when comparing the scattering from pure apoferritin diluted in AMPSO buffer at room temperature with the same apoferritin heated at 65 °C for 100 min. It should be noted that without high-temperature treatment magnetite/maghemite will not be formed in the protein cavity, and without magnetite/maghemite the magnetic susceptibility of MFer will be very low. The mechanisms of iron core formation in magnetoferritin includes the mineralization of iron oxides inside apoferritin shell using controlled thermal oxidation conditions. This process could be similar to the formation of an inorganic nucleus in physiological ferritin[14] and can be summarized in four main steps: Fe^{2+} ions input, Fe^{2+} oxidation to Fe^{3+}, nucleation and growth of inorganic nucleus[15].

Many works confirmed, that iron accumulation and presence of magnetite crystals in pathological ferritin can be the reason of various diseases development[16-17]. In recent years, great emphasis has been put on early diagnosis of these diseases using various techniques as magneto-optical or magnetic resonance imaging (MRI) measurements. Magnetoferritin, prepared at extreme conditions such as high temperature which insure formation of magnetite/maghemite nanoparticles and high LF should increase the hypointensive artefacts in MRI. Such findings are highly promising for exploiting the use of magnetoferritin as a noninvasive diagnostics tool of pathological processes, where the magnetoferritin particles could be utilised as MRI iron quantification standards[18-22].

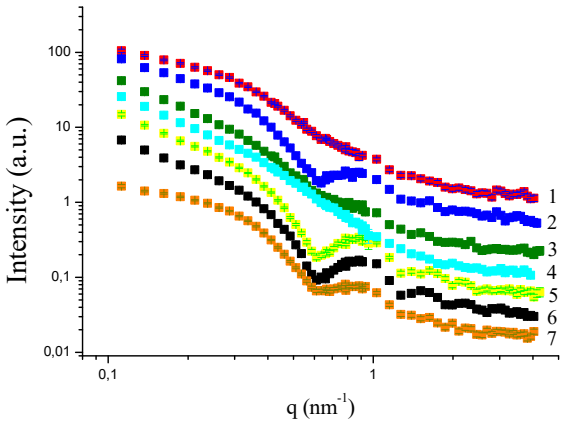

Figure 2 SANS curves of magnetoferritin (MFer) samples prepared at various synthesis temperatures with different loading factors in comparison with apoferritin. (1) apoferritin heated at 65°C for 100 min, (2) MFer with LF 940 prepared at 75°C, (3) MFer with LF 660 prepared at 65°C, (4) MFer with LF 810 prepared at 55°C, (5) MFer with LF 640 prepared at 37°C, (6) MFer with LF 730 prepared at 23°C, (7) pure apoferritin solution.

SAXS experiments were performed on samples prepared with lower LF (270 - 280). At such loading, the oscillations of the scattering form-factor are more pronounced, the particle agglomeration is relatively weak, and the scattering from the magnetic nanoparticles also weak. Therefore, the effect of the synthesis temperature on the MFer structure can be observed more clearly. Indeed, Figure 3 shows a gradual smoothing of the scattering curves with an increase in the synthesis temperature, indicating the decomposition of the core-shell structure of apoferritin by increasing of preparation temperature.

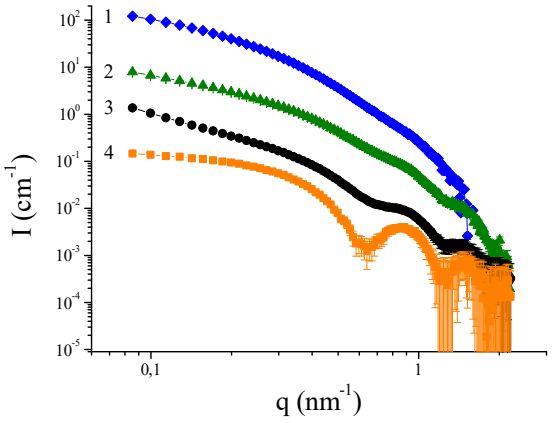

Figure 3 SAXS curves for MFer samples with similar loading factors prepared at different temperatures in comparison with pure apoferritin. (1) LF 270 prepared at 75°C, (2) LF 270 prepared at 65°C, (3) LF 280 prepared at 23 °C and (4) pure apoferritin.

Such synthesis temperature dependent variation of the core-shell structure was not studied until now for magnetoferritin. It is generally known that the protein undergoes structural changes under the influence of temperature, the most significant changes occurring at the denaturation limit, where the protein loses its functionality and the spatial arrangement of the peptide chain. Similar variation of magnetoferritin structure was also observed in

previous works under the influence of different loading factors[9-11] and pH[12]. From our study we can conclude, that the synthesis temperature plays a crucial role in forming the protein structure and magnetic properties, and has to be taken into account for future applications of magnetoferritin in biomedical imaging.

4. Conclusions

In this study, we observed structural differences in the protein shell integrity and a change of the magnetic properties of the metallic core of MFer as a function of synthesis temperature. Besides revealing the mechanism of formation of the magnetic core, the data provided a way to optimize the synthesis process, i. e., to achieve better structural stability and higher magnetization of the material. Our investigations show that low synthesis temperatures lead to the formation of stable core-shell structures, while higher temperatures result in samples with higher magnetization. Therefore, for obtaining good structural and magnetic properties, a compromise should be found. The present results indicate that the optimal temperature for MFer synthesis is between 55-65°C and LF is below 600. Magnetoferritin with higher magnetization should be prepared with high LF above 600 at temperatures near protein denaturation point. These conditions ensure favorable physical properties, i.e. strong contrast and sufficient colloidal stability, suitable for biomedical imaging applications.

This work was supported by the project of the Slovak Scientific Grant Agency VEGA (project No. 2/0016/17 and No. 2/0062/16), the Slovak Research and Development Agency under the contract No. APVV-015-0453, by the Agency of the Ministry of Education, Science, Research and Sport of the Slovak Republic for the Structural Funds of EU (projects No. 26210120012 and No. 26220220186) and by the MAGBBRIS project Euronanomed III.

Online Supplementary Materials
Supplementary data associated with this article can be found in the online version at doi:

References

1 G. Jutz, P. van Rijn, B. Santos Miranda, A. Böker, *Chem. Rev.,* 2015, **115**, 1653.
2 F. C. Meldrum, T. Douglas, S. Levi, P. Arosio, S. Mann, *J. Inorg. Biochem.,* 1995, **58**, 59.
3 T. Douglas, V. T. Stark, *Inorg. Chem.,* 2000, **39**, 1828.
4 F. C. Meldrum, B. R. Heywood, S. Mann, *Science*, 1992, **257**, 522.
5 E.C. Theil, R. K. Behera, T. Tosha, Coord. *Chem. Rev.,* 2013, **257**, 579.
6 S. Stefanini, S. Cavallo, C. Q. Wang, P. Tataseo, P. Vecchini, A. Giartosio, E. Chiancone. *Arch. Biochem. Biophys.,* 1996, **325**, 58.
7 K. K. W. Wong, T. Douglas, S. Gider, D. D. Awschalom, S. Mann, *Chem. Mater.,* 1998, **10**, 279.
8 M. J. Martínez-Pérez, R. de Miguel, C. Carbonera, M. Martínez-Júlvez, A. Lostao, C. Piquer, C. Gómez-Moreno, J. Bartolomé, F. Luis, *Nanotechnology*, 2010, **21**, 465707.
9 L. Melnikova, V. I. Petrenko, M. V. Avdeev, V. M. Garamus, L. Almásy, O. I. Ivankov, L. A. Bulavin, Z. Mitróová, P. Kopčanský, *Coll. Surf. B,* 2014, **123**, 82.
10 L. Melnikova, V. I. Petrenko, M. V. Avdeev, O. I. Ivankov, L. A. Bulavin, V. M. Garamus, L. Almásy, Z. Mitroova, P. Kopcansky, *J. Magn. Magn. Mater.,* 2015, **377**, 77.
11 L. Melníková, Z. Mitróová, M. Timko, J. Kováč, M. V. Avdeev, V. I. Petrenko, V. M. Garamus, L. Almásy, P. Kopčanský. *Mendeleev Commun.,* 2014, **24**, 80.

12 L. Balejčíková, V. M. Garamus, M. V. Avdeev, V. I. Petrenko, L. Almásy, P. Kopčanský, *Coll. Surf. B*, 2017, **156**, 375.
13 J. M. Cowley, D. E. Janney, R. C. Gerkin, P. R. Buseck, *J. Struct. Biol.,* 2000, **131**, 210.
14 U. M. D. Testa, Proteins of iron metabolism. 1. ed. USA: Informa Healthcare, 2001.
15 A. M. Koorts, M. Viljoen, Acute Phase Proteins: Ferritin and Ferritin Isoforms, in: Acute Phase Proteins - Regulation and Functions of Acute Phase Proteins. p. 153, edited by Francisco Veas, China: IntechOpen, 2011.
16 M. A. Smith, P. L. R. Harris, L. Sayre, G. Perry, *Proc Natl Acad Sci U S A,* 1997, **94**, 9866.
17 J. Dobson, *FEBS Lett.,* 2001, **496**, 1.
18 J. W. Bulte, T. Douglas, S. Mann, R. B. Frankel, B. M. Moskowitz, R. A. Brooks, C. D. Baumgarner, J. Vymazal, J. A. Frank, *Invest Radiol.*, 1994, **29**, 214.
19 J. W. Bulte, T. Douglas, S. Mann, R. B. Frankel, B. M. Moskowitz, R. A. Brooks, C. D. Baumgarner, J. Vymazal, M. P. Strub, J. Frank, *J. Magn. Reson. Imaging*, 1994, **4**, 497.
20 V. C. Jordan, M. R. Caplan, K. M. Bennett, *Magn. Reson. Med.,* 2010, **64**, 1260.
21 Y. Zhao, M. Liang, X. Li, K. Fan, J. Xiao, Y. Li, H. Shi, F. Wang, H. S. Choi, D. Cheng, X. Yan, *ACS Nano*, 2016, **10**, 4184.
22 O. Strbak, L. Balejcikova, L. Baciak, J. Kovac, M. Masarova-Kozelova, A. Krafcik, D. Dobrota, P. Kopcansky, *J. Phys. D: Appl. Phys.,* 2017, **50**, 365401.